

The Effect Of Wave Length And Amplitude on The Hydrodynamic Characteristics of Waste Collection Vessels Using *Computational Fluid Dynamics (CFD)*

Erik Sugianto¹, Hadi Prasutiyon¹, Arif Winarno¹, Muhammad Khasroni Hamsah¹

(Received: 10 February 2023 / Revised: 22 February 2023 / Accepted: 05 March 2023)

Abstract— The continuous flow of marine debris in the sea has been a problem until now. Previous research on garbage collection vessels was conducted in calm water conditions, without waves and waves due to wind. This is different from the real conditions in the sea which are choppy and bumpy. In addition, research on the effect of wave length and amplitude on marine debris collection on garbage collection vessels does not yet exist. This study aims to determine the effect of wave length and amplitude on velocity contours, flow patterns, and ship resistance. The ship uses a circular hollow wing conveyor. Modelling using *Rhinoceros software*, then numerical simulation using *Computational Fluid Dynamic (CFD)*. Verification of the simulation process uses *grid independent* by varying the *mesh size*, then validation of the results is done by comparing with previous experimental research. The results show that the best velocity contour in front of the conveyor is at a ship speed of 1.028 m/s (2 knots) using an amplitude of 0.5 T and a wavelength of 0.5 L. The velocity value in front of the conveyor is 1.551 m/s. This affects the speed of collecting marine debris. This affects the speed of collecting marine debris. The model that has a laminar flow pattern at the bow and at the stern is a speed of 1 knot at an amplitude variation of 0.1 T and a wavelength of 0.1 L. This is the best because it is easy to collect garbage. The smallest drag is the speed of 0.514 m/s (1 knot) at amplitude variation of 0.1 T and wavelength of 0.1 L. At this condition, the fuel consumption is the least. Thus, the greater the wavelength and amplitude of the waves the greater the drag and the smaller the speed.

Keywords: Garbage collection vessel, marine debris, wavelength, wave amplitude.

I. INTRODUCTION

Marine debris that continues to flow in the sea is a problem to this day [1]. The size of marine debris varies from very small in micrometres, a few centimetres, such as plastic bags and soda bottles, to the largest in size of tens of metres, such as shipwrecks and lost containers [2]. Based on the amount of ocean in 2010, it is estimated that from these conditions, the total plastic mass in 2025 will increase from 100 to 250 million tonnes under the same commercial assumptions [3]. Communities around seas and rivers have a significant influence on this content [4]. Then the involvement and utilisation of the community around the sea and river by using digital technology is also possible to overcome this problem [5].

Research on catamaran hull type on marine waste collection behaviour. This research focuses on the effect of catamaran hull face shape on waste collection in still water through numerical methods. The three front hull variations used were symmetrical hull type, inner flat, and outer flat. It was carried out using

speed variations of 1 to 4 knots. The results showed that inner flat hull 4 catamaran has the smallest total resistance value compared to others [6]. Garbage collection and cleaning technologies began to emerge and continue to develop [7]. A small boat with a garbage collection system was proposed [8]. Furthermore, research on the effect of the shape of the holes in the *conveyor* wing on the effectiveness in garbage collection was conducted [9]. However, the ship has not been added to the research. Then, research on the variation of *conveyor* location was conducted [10].

The result is that the location of the *conveyor* at the bow is the choice, the selection is based on a smaller resistance value having a flow pattern close to the *conveyor* which indicates that the ship will quickly collect garbage. Furthermore, catamaran vessels are superior compared to *monohull* vessels in terms of collecting waste. This is because catamaran vessels are faster and easier to collect waste compared to *monohull vessels* [11]. However, the catamaran ship does not have a *wing conveyor* installed.

Erik Sugianto is Assistant Professor of Department of Marine Engineering, Universitas Hang Tuah, Surabaya, Indonesia.
E-mail: erik.sugianto@hangtuah.ac.id
Hadi Prasutiyon is Assistant Professor of Department of Marine Engineering, Universitas Hang Tuah, Surabaya, Indonesia.
E-mail: hadi.prasutiyon@hangtuah.ac.id

Arif Winarno is Assistant Professor of Department of Marine Engineering, Universitas Hang Tuah, Surabaya, Indonesia.
E-mail: arif.winarno@hangtuah.ac.id
Muhammad Khasroni Hamsah is student of Department of Marine Engineering, Universitas Hang Tuah, Surabaya, Indonesia.
E-mail: m.k.hamsah44@gmail.com

Research on catamaran vessels and the use of *wing conveyors* was conducted [12]. The results show that *wing conveyors* with circular hollow wings are superior in collecting marine debris. The shape of the *wing conveyor* causes the garbage to easily and quickly approach the ship. However, all of the above studies were conducted in calm water conditions, without waves and waves caused by wind.

This is different from the real conditions in the seawhich are choppy and bumpy. In addition, there is no research on the effect of wave length and amplitude on marine debris collection on garbage collection vessels. Therefore, this study proposes to investigate the effect of wave length and amplitude on the hydrodynamic characteristics of a garbage collection vessel using *Computational Fluid Dynamics (CFD)*.

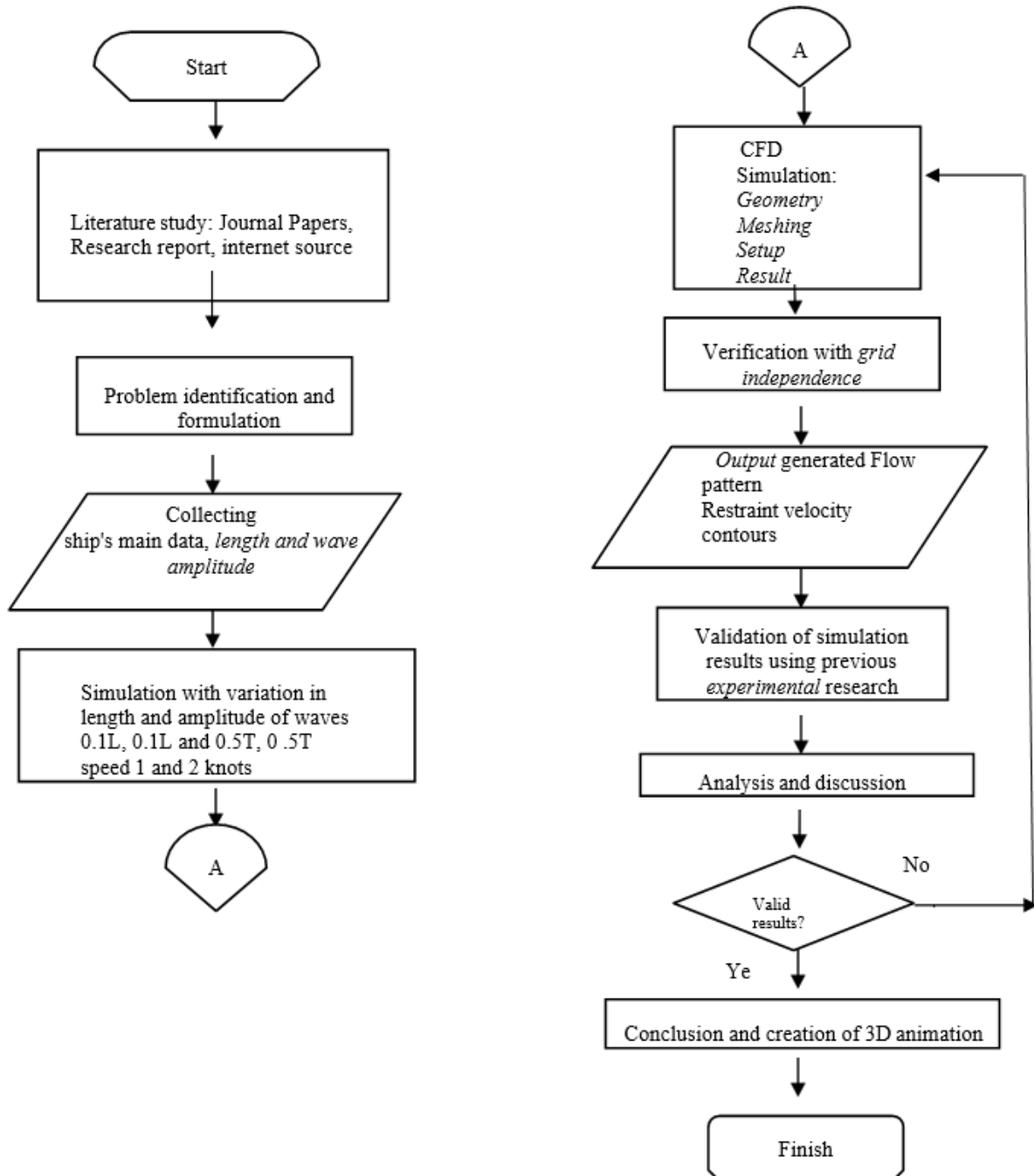


Figure 1. Research flowchart

II. RESEARCH METHODS

The method used in this research is a numerical method, namely using *Ansys fluent software* on a circular hollow wing model. The purpose of the research is to get the optimal speed contour, flow pattern, ship resistance for the garbage collection process. The steps of the research process carried out in the research are shown in Figure 1.

This study aims to determine the effect of length and amplitude of waves on velocity contours, flow patterns, total resistance. Velocity contours will affect how fast marine debris can approach the ship and flow patterns affect the total resistance. how easily marine debris approaches the ship. Modelling was done using *Maxsurf software*, then numerical simulation was done using *CFD*. Verification is done with *grid independence* and validation is done with the results of previous similar research *experiments*. Furthermore, ship resistance will affect the fuel consumption and

emissions produced by the ship.

2.1. Data Collection

This stage is carried out the process of collecting data taken from previous research [11]. The main ship size data of the waste collection ship obtained was modeled using a plugin in Rhyno, then surface in export to Ansys Fluent as an *x_t* file. After converting the *geometry to mesh*, the tightness of the *geometry* was also checked.

This is used to clearly define the length of the conveyor and to ensure the exceedance of the nose ship. Furthermore, it will be processed into *Rhinoceros software* and continued using *CFD* simulation using *Ansys software*. The following are the main ship sizes and ship types in Table 1. This stage is carried out the process of collecting data taken from BMKG maritime Tanjung Perak Surabaya. For the blue colour, the wave height result is 3 m and for the blue colour, and for orange color shows the highest result obtained with a value of 10 m. The following wave height graph in Figure 2.

TABLE 1.
 MAIN SHIP SIZE DETAILS [11]

| Parameters | Symbol | Catamaran |
|-----------------------------------|----------------|-----------|
| Overall length (m) | Loa | 4,000 |
| Perpendicular length (m) | Lpp | 3,950 |
| Waterline length (m) | Lwl | 3,858 |
| Maximum width (m) | B | 1,200 |
| Height (m) | H | 0,600 |
| Draft (m) | T | 0,300 |
| Wet surface area (m) ² | WSA | 5,723 |
| Conveyor length (m) | Lc | 1,625 |
| Conveyor angle (hi) | La | 20 |
| Conveyor width (m) | Lw | 0,600 |
| Volume displacement | M ³ | 0,36 |
| Block coefficient | - | 0,25 |

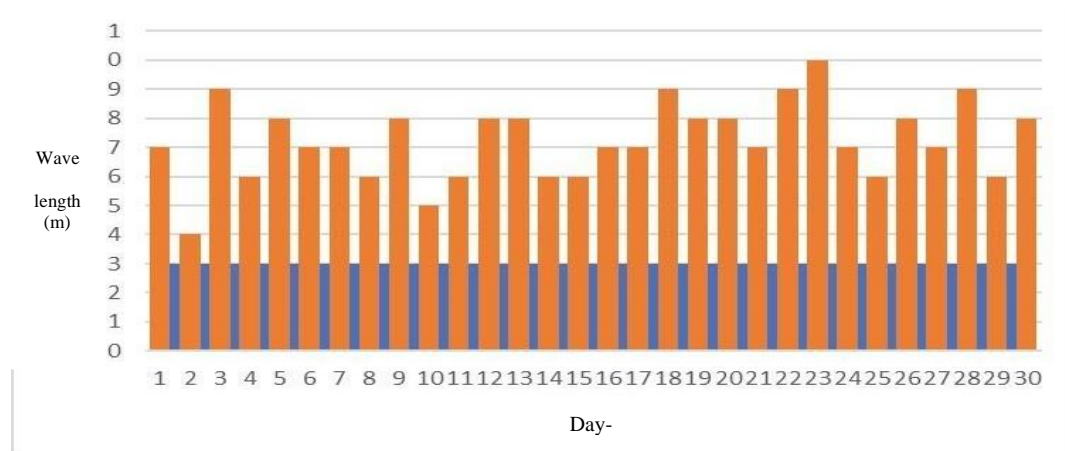


Figure 2. Data of wave in Surabaya Sea [13]



Figure 3. Winged conveyor with *solid* wings



Figure 4. Winged conveyor with *oval* hole wing



Figure 5. Winged conveyor with *circle* hole wing

2.2. Modelling

Modeling of the catamaran ship, wing and conveyor using *maxsuft* software which is then converted to *Computational Fluid Dynamic (CFD)* format. The hull model that will be made is based on the limitations of the problem that has been determined. The following in Figure 3 shows the solid model of the length of the conveyor is 370 mm and the conveyor width is 180 mm.

Figure 4 shows the oval model of the length of the conveyor is 370 mm and the width of the conveyor is 180 mm. Figure 5 shows circle model of the length of the conveyor is 370 mm and the width of the conveyor is 180 mm. *Conveyor* model with 3 wing variations on an *inner flat bottom* catamaran ship. After making the model, the model was *converted* to *Ansys* software. The next step is model simulation and data recording. Model simulation was performed on *Computational FluidDynamic (CFD)*.

2.3. Geometry

The geometry process is an *import* process of the ship model that has been made with *Rhino* 6 software before then converted into *Ansys* software. Figure 6. is the *geometry* with variations in the shape of the circle hole. L1 shows the results of the distance of the starboard part of the ship in the pool, which is $2.5 \times \text{ship length} = 2.5 \times 4000 \text{ mm} = 10000 \text{ mm}$. L2 shows the distance of the bow of the ship in the pool which is $2.5 \times \text{ship length} = 2.5 \times 4000 \text{ mm} = 10000 \text{ mm}$.

L3 shows the results of the distance of the stern of the ship in the pool, namely $3 \times \text{Ship length} = 3 \times 4000 \text{ mm} = 12000 \text{ mm}$. L4 shows the result of the stern section in the pool which is $4 \times \text{Ship length} = 4 \times 4000 \text{ mm} = 16000 \text{ mm}$. FD1 shows the results of the distance of the upper part of the ship in the pool which is $1 \times \text{Ship length} = 1 \times 4000 \text{ mm} = 4000 \text{ mm}$. FD2 shows the results of the distance of the downstream part of the ship on the pool which is $2 \times \text{Ship length} = 2 \times 4000 \text{ mm} = 8000 \text{ mm}$ [11].

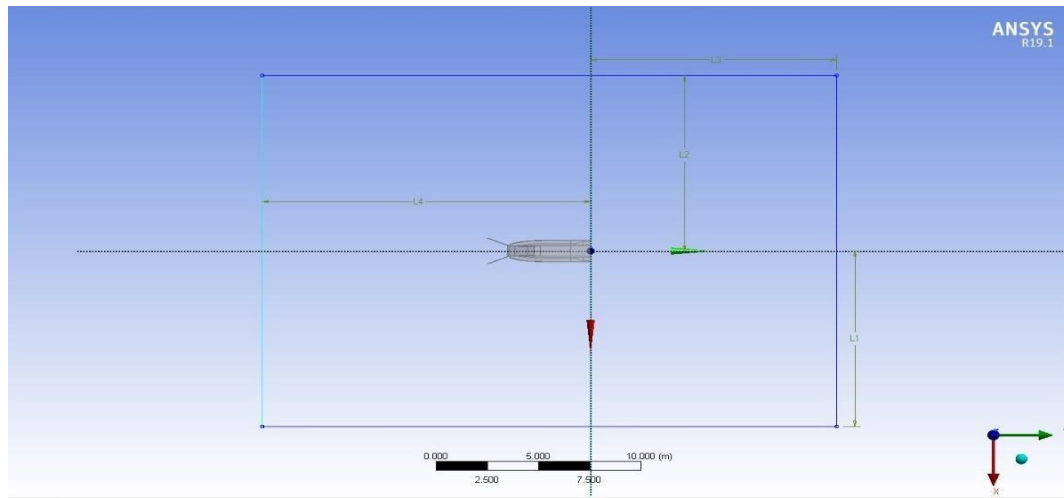


Figure 6 Pool Geometry of a conveyor vessel with hollow wings

2.4. Meshing

The meshing process is the arrangement of components into small elements to determine the character of a ship shape that will be analysed. At this meshing stage, the addition of boundaries such as inlet which is defined as the direction of fluid flow, outlet which is defined as the direction of fluid flow exit, wall defined as the right and left side pool boundaries, and hull defined as the body of the ship that affects fluid flow. The following are the meshing results of the conveyor ship model with a circular hollow wing variation in Figure 7. shows the meshing results with a body sizing of 500 mm, face sizing of 400 mm, and an inflation mesh of 15 layers which produces 796409 elements using meshing type

tetrahedrons, in Figure 8. shows the results of meshing with body sizing 300 mm, face sizing 150 mm and inflation mesh as many as 15 layers which produces 2307989 elements using meshing with tetrahedrons, in Figure 9. shows the results of meshing with body sizing 400 mm, face sizing 200 mm and inflation mesh as many as 15 layers which produces 1055135 elements using meshing with tetrahedrons and in Figure 10. shows the results of meshing with body sizing 350 mm, face sizing 250 mm and inflation mesh as many as 15 layers which produces 1633329 elements using meshing with tetrahedrons.

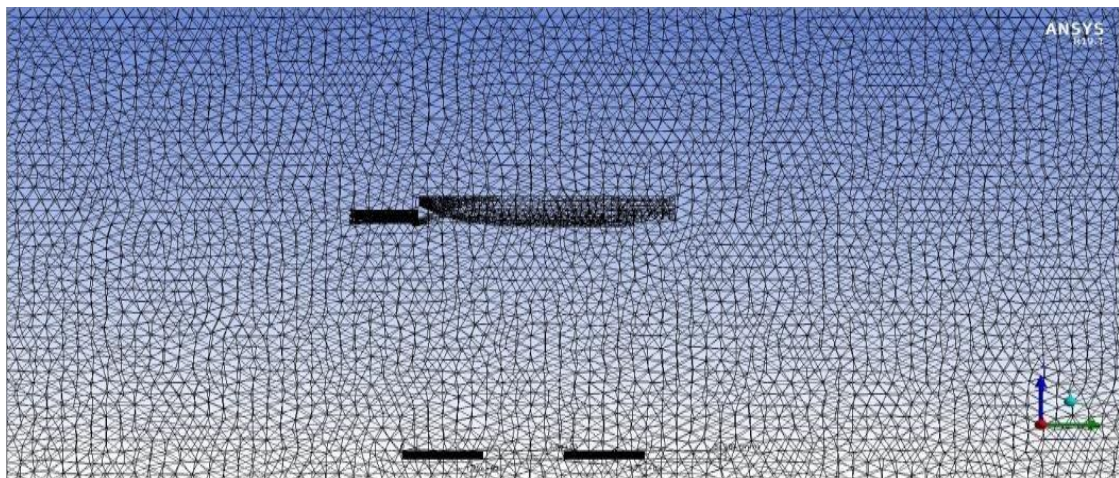


Figure 7. Meshing results of body sizing 500 mm, face sizing 400 mm

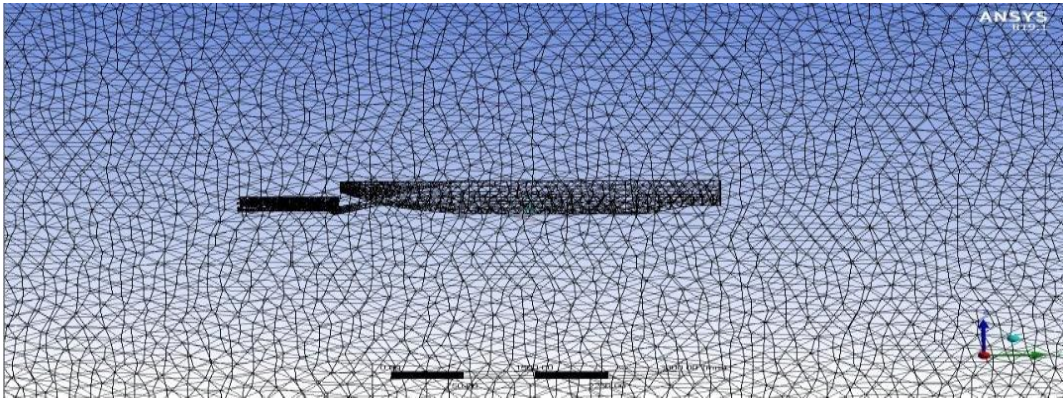


Figure 8. Meshing results of body sizing 300 mm, face sizing 150 mm

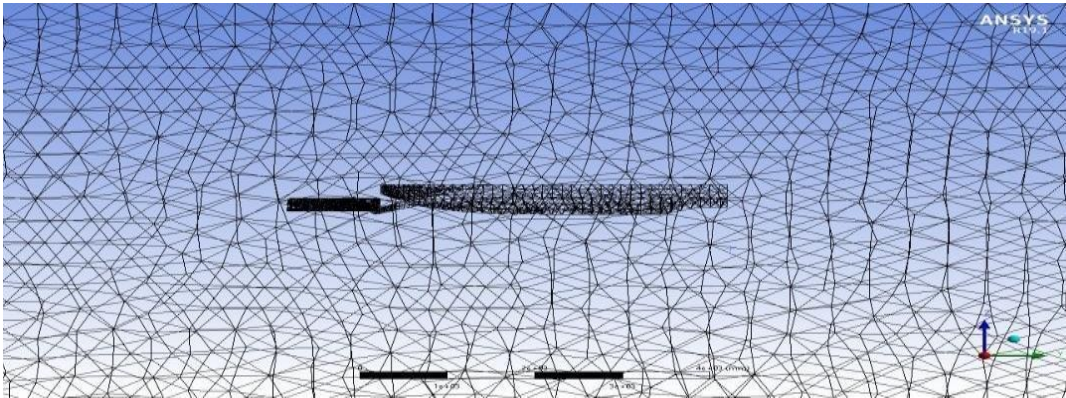


Figure 9. Meshing results of body sizing 400 mm, face sizing 200 mm

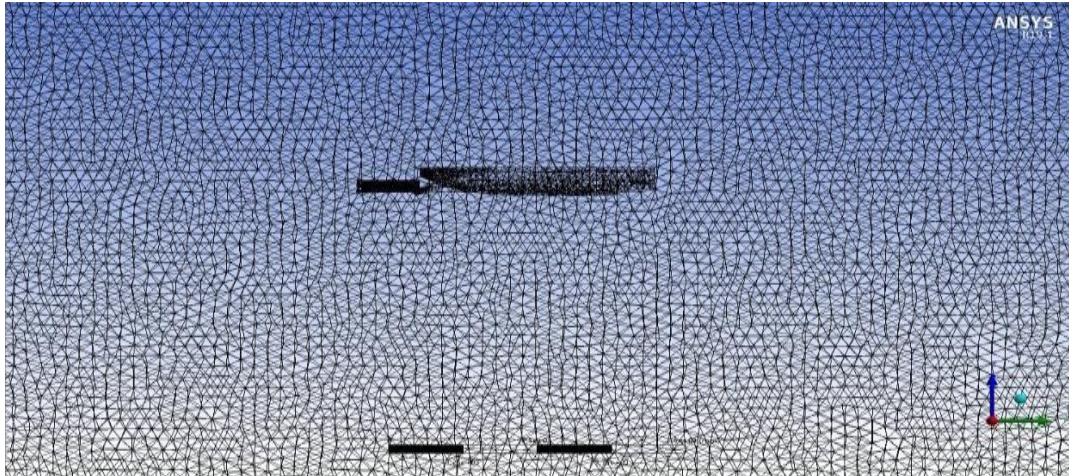


Figure 10. Meshing results of body sizing 350 mm, face sizing 250 mm

2.5. Set up

This process is the most important process because almost all parameters are processed in this stage. *The set-up* process must also fulfil the

convergence of the calculated stages. Here are some things that need to be *set up* first to perform the *set up* in Table 2.

TABLE 2
 SETTINGS DURING THE SET-UP PROCESS

| Processing option | parallel |
|----------------------|--|
| Processor | 8 |
| Type | Steady prepressure base |
| Gravity | Z: -9.81 m/s^2 |
| Vicous | k-epsilon (2 eqn), standard |
| Multiphase | volume of fluid, open channel flow, implicit, implicit body force |
| Phase 2 | water liquid |
| Material | water liquid |
| Inlet | Boundary conditions multiphase |
| bottom level | -8 m |
| Monitor | Residual, report plot, force report, drag, drag force, hull |
| Initialisation | standard initialisation, from inlet |
| Timescale factor | Run calculation 0.5 |
| Number of iterations | 500 |

The following are the results of the *set-up* process of the conveyor ship model with variations in the shape of the circular hole. Figure 11 shows the *set-up* results with *body sizing* 500 mm, *face sizing* 400 mm, and *inflation mesh* of 15 layers resulting in 796409 elements using *tetrahedrons* type *meshing*. Starting to converge since iteration 70, in Figure 12. shows the *meshing* results with *body sizing* 300 mm, *face sizing* 150 mm and *inflation mesh* as many as 15 layers which produces 2307989 elements using *meshing* with *tetrahedrons*. Started to converge since iteration 200.

Figure 13. shows the *meshing* results with *body sizing* 400 mm, *face sizing* 200 mm and *inflation mesh* of 15 layers which produces 1055135 elements using *meshing* with *tetrahedrons*. Started to converge since 100 and in Figure 14. shows the *meshing* results with *body sizing* 350 mm, *face sizing* 250 mm and *inflation mesh* as many as 15 layers which produces 1633329 elements using *meshing* with *tetrahedrons*. Started to converge since iteration 140. Shows the *set-up* stage with a speed variation of 1 knot. With convergence achieved at 500 iterations.

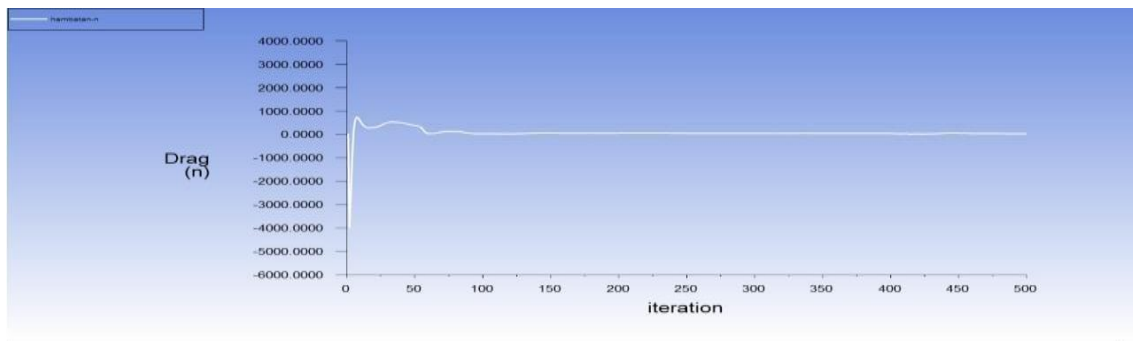


Figure 11. Iteration solution of body sizing 500 mm, face sizing 400 mm

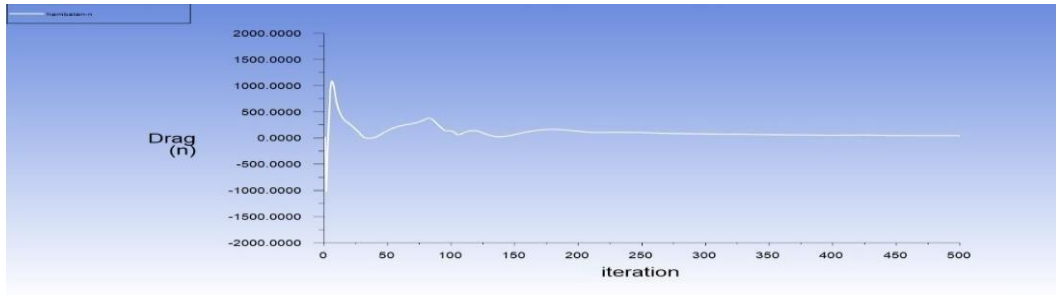


Figure 12. Iteration solution of body sizing 300 mm, face sizing 150 mm

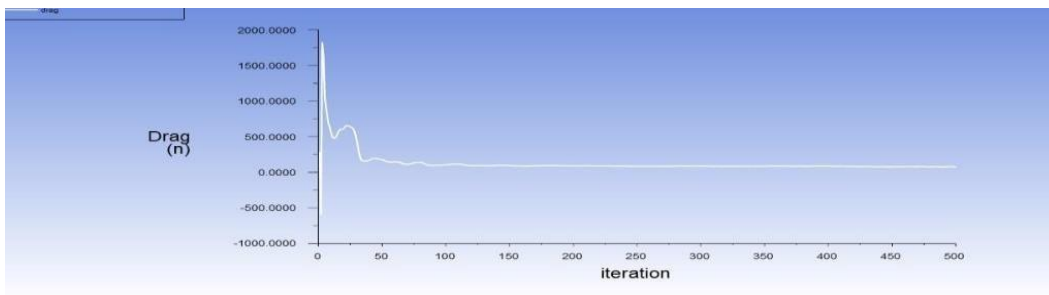


Figure 13. Iteration solution of body sizing 400 mm, face sizing 200 mm

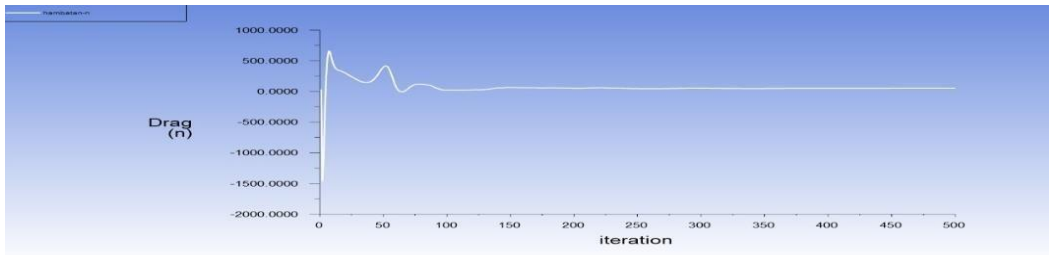


Figure 14. Iteration solution of body sizing 350 mm, face sizing 250 mm

III. RESULTS AND DISCUSSION

Result is the final stage after the *set-up* process has been carried out and a visual of the model under study is obtained. In this research, the result will display the velocity contours associated with the model, how fast the ship can approach the debris, the flow pattern itself is used for how easily the marine debris approaches the ship, the resistance is used to determine the fuel consumption.

3.1 Verification Process with Grid Independence

Verification is done using *grid independence* to verify that the mesh used is correct. This ensures that when if the mesh settings are slightly changed, it will not affect the simulation results. The following are the results of *grid independence* verification in Table 3.

TABLE 3.
 VARIATION OF MESHING RESULTS

| speed | | Body sizing | Face sizing | Number of elements | Resistance (N) |
|--------|-----------|-------------|-------------|--------------------|----------------|
| 1 knot | 0.514 m/s | 500 | 400 | 796409 | 1.553 |
| 1 knot | 0.514 m/s | 300 | 150 | 2307989 | 2.157 |
| 1 knot | 0.514 m/s | 400 | 200 | 1055135 | 1.723 |
| 1 knot | 0.514 m/s | 350 | 250 | 1633329 | 2.561 |

Figure 15 shows the comparison of the number of meshing elements of the four simulations with the total resistance of the ship. The results show that the

Independent Grid shows a difference of 14.16%. This is acceptable because is still below 15% and the mesh size used for further research is *Body sizing* 350 and *Face sizing* 250.

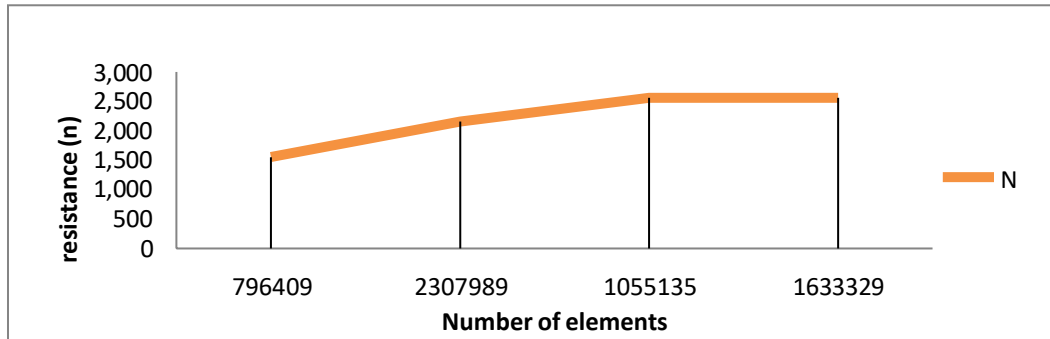


Figure 15. Meshing variation graph

3.2. Effect of Wave Length and Amplitude on the Speed Contour of the Garbage Collection Vessel

Figure 16. shows the results of the velocity contours with two wave variations of 0.1 T, 0.1 L and 0.2 L. 0.5 T, 0.5 L with two speed variations 0.514 m/s (1 knot) and 1.028 m/s (2 knots). (a) speed of 0.514 m/s (1 knot) with wave variations of 0.1 T and 0.1L.

Figure 16. (b) speed of 0.514 m/s (1 knot) with wave variations of 0.1 T and 0.1L. Figure 16 (c) speed of 1.028 m/s (2 knots) with variations of 0.5 T and 0.5 L waves. Figure 16. (a) shows the results of the fluid flow velocity contours marked (.) in front of the bow and near the wing. In front of the bow of 0.7 m / s. The colour contour of the fluid velocity is blue to red, the more the colour approaches the top red, the higher the speed value.

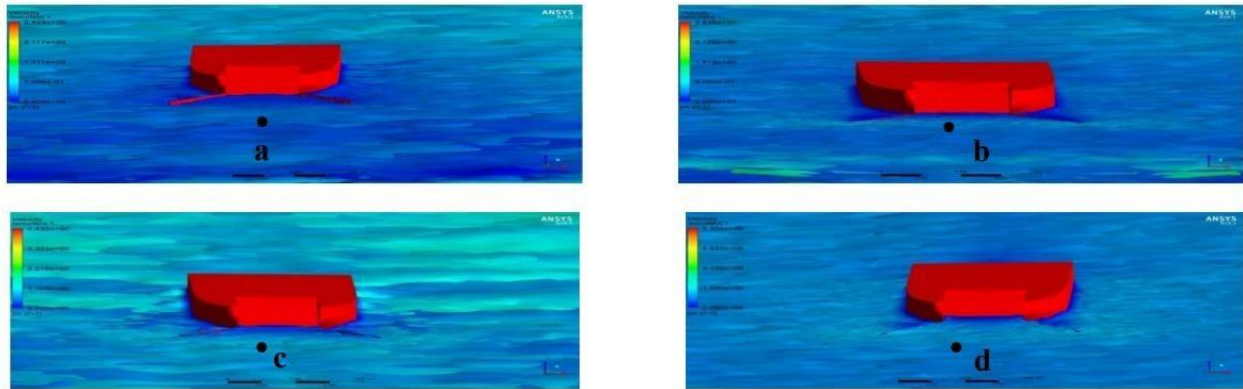


Figure 16 Front view of velocity contours (a) 0.1 T, 0.1 L at 1 knot (b) 0.5 T, 0.5 L at 1 knot (c) 0.1 T, 0.1 L at 2 knots (d) 0.5 T and 0.5 L speed 2 knots.

From Figure 16. (a) it is known that the velocity in front of the conveyor at an amplitude of 0.1 T and a wavelength of 0.1 L with a speed of 5.14 m/s (1 knot) is 0.7 m/s. Figure 16. (b) shows that in front of the conveyor at an amplitude of 0.5 T and a wavelength of 0.5 L with a speed of 5.14 m/s (1 knot) is 0.9 m/s. Figure 16. (c) shows that in front of the conveyor at an amplitude of 0.1 T and 0.1 L with a speed of 1.028 m/s (2 knots) is 0.9 m/s (2 knots) is 1.108 m/s. Figure 16. (d) shows that in front of the conveyor at an amplitude of 0.5 T and a wavelength of 0.5L with a speed of 1.028 m/s (2 knots) is 1.551 m/s (2 knots). So that under the condition of amplitude 0.5 T and a wavelength of 0.5 L at a speed of 1.028 m/s (2 knots) is 1.551 m/s the fastest condition in collecting waste.

Figure 16 shows the results of the velocity contours with two wave variations of 0.1 T, 0.1 L and 0.1 L. 0.5 T, 0.5 L with two speed variations 0.514 m/s (1 knot) and 1.028 m/s (2 knots). (a) speed of 0.514 m/s (1 knot) with wave variations of 0.1 T and 0.1L. Figure 17. (b) speed of 0.514 m/s (1 knot) with wave variations of 0.5 T and 0.5 L. Figure 17. (c) speed of 1.028 m/s (2 knots) with wave variations of 0.5 T and 0.5 L. Figure 17. (d) speed of 1.028 m/s (2 knots) with wave variations of 0.5 T and 0.5 L. From Figure 17. (b) shows the results of fluid flow velocity contours marked (.) in front of the bow and near the wing. In front of the bow of 0.9 m / s. The colour contour of the fluid velocity is blue to red, the more the colour approaches the top red, the higher the speed value.

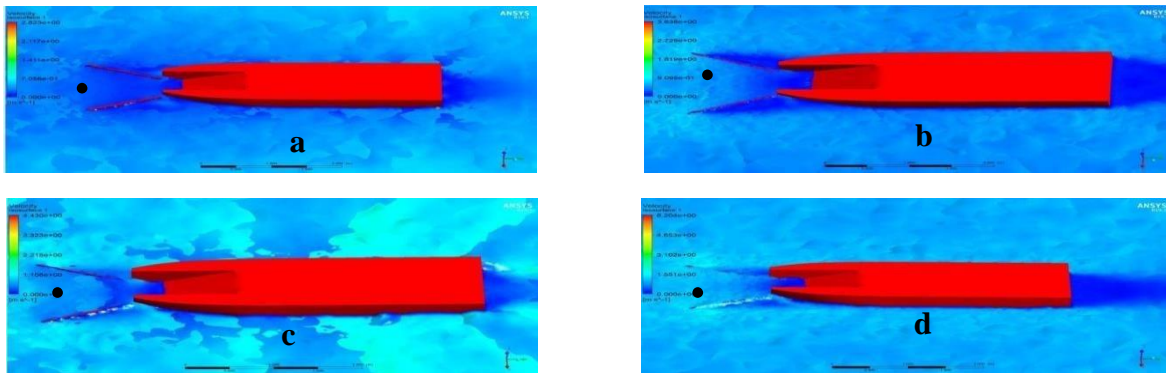


Figure 17. Top view of velocity contours (a) 0.1 T, 0.1 L at 1 knot (b) 0.5 T, 0.5 L at 1 knot (c) 0.1 T, 0.1 L at 2 knots (d) 0.5 T and 0.5 L speed 2 knots.

From Figure 17. (a) it is known that the velocity in front of the conveyor at an amplitude of 0.1 T and a wavelength of 0.1 L with a speed of 5.14 m/s (1 knot) is 0.7 m/s. Figure 17. (b) shows that in front of the conveyor at an amplitude of 0.5 T and a wavelength of 0.5 L with a speed of 5.14 m/s (1 knot) is 0.9 m/s. Figure 17. (c) shows that in front of the conveyor at an amplitude of 0.1 T and 0.1 L with a speed of 1.028 m/s (2 knots) is 0.9 m/s (2 knots) is 1.108 m/s. Figure 17. (d) shows that in front of the conveyor at an amplitude of 0.5 T and a wavelength of 0.5 L with a speed of 1.028 m/s (2 knots) is 1.551 m/s (2 knots). So that under the condition of amplitude 0.5 T and a wavelength of 0.5 L at a speed of 1.028 m/s (2 knots) is

1.551 m/s the fastest condition in collecting waste.

Figure 18. shows the results of the velocity contours with two wave variations of 0.1 T, 0.1 L and 0.5 T, 0.5 L with two speed variations 0.514 m/s (1 knot) and 1.028 m/s (2 knots). (a) speed of 0.514 m/s (1 knot) with wave variations of 0.1 T and 0.1 L. (b) speed of 0.514 m/s (1 knot) with wave variations of 0.5 T and 0.5 L. (c) speed of 1.028 m/s (2 knots) with wave variations of 0.5 T and 0.5 L. Figure 18. (d) speed of 1.028 m/s (2 knots) with wave variations of 0.5 T and 0.5 L. From Figure 18. (c) shows the results of fluid flow velocity contours marked (.) in front of the bow and near the wing. In front of the bow of 1.108 m/s. The colour contour of the fluid velocity is blue to red, the more the colour approaches the top red, the higher the speed value.

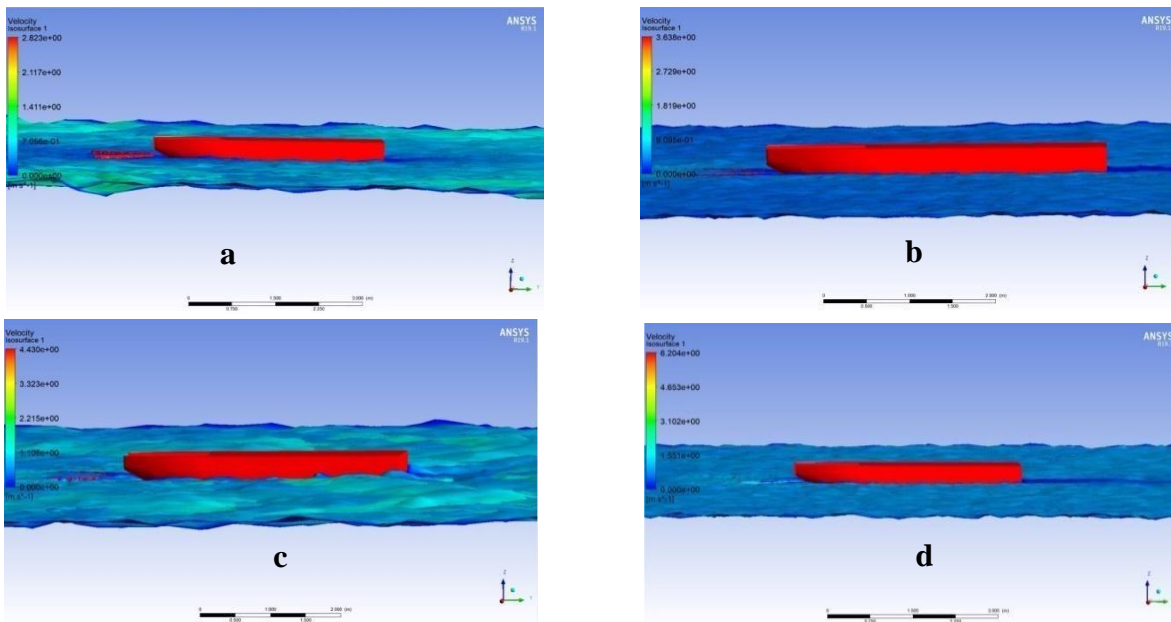


Figure 18 Side view of velocity contours (a) 0.1 T, 0.1 L at 1 knot (b) 0.5 T, 0.5 L at 1 knot (c) 0.1 T, 0.1 L at 2 knots (d) 0.5 T and 0.5 L at 2 knots

From Figure 18. (a) it is known that the velocity in front of the conveyor at an amplitude of 0.1 T and a wavelength of 0.1 L with a speed of 5.14 m/s (1 knot) is 0.7 m/s. Figure 18. (b) shows that in front of the conveyor at an amplitude of 0.5 T and a wavelength of 0.5 L with a speed of 5.14 m/s (1 knot) is 0.9 m/s. Figure 18. (c) shows that in front of the conveyor at an amplitude of 0.1 T and 0.1 L with a speed of 1.028 m/s (2 knots) is 0.9 m/s (2 knots) is 1.108 m/s. Figure 18. (d) shows that in front of the conveyor at an amplitude of 0.5 T and a wavelength of 0.5L with a speed of 1.028 m/s (2 knots) is 1.551 m/s (2 knots). So that under the condition of amplitude 0.5 T and a wavelength of 0.5 L at a speed of 1.028 m/s (2knots) is 1.551 m/s the fastest condition in collectingwaste.

3.3 Comparative analysis of velocity 5.014 m/s (1 knot) and 1.028 m/s (2 knots) with two wave variations 0.1 T, 0.1 L and 0.5 T, 0.5 L

From Figure 19 is comparison of speed with two wave variations in Figure 19. (a). velocity 0.514 m/s (1 knot), Figure 19. (b). velocity 0.514 m/s (1 knot), Figure 19. (c). speed of 1.028 m/s (2 knot). Figure 19 (d). speed of 1.028 m/s (2 knots). From Figure 19 (d) it can be analysed that the best velocity contour is at a speed of 1.028 m/s (2 knots). From the analysis of the circular hollow wing with amplitude variation of 0.5 T and wavelength of 0.5 L has the highest velocity contour with a value of 1.551 m/s at the bow and aft.

From Figure 19. (a) it is known that the velocity in front of the conveyor at an amplitude of 0.1 T and a wavelength of 0.1 L with a speed of 5.14 m/s (1 knot) is 0.7 m/s. Figure 19. (b) shows that in front of the conveyor at an amplitude of 0.5 T and a wavelength of

0.5 L with a speed of 5.14 m/s (1 knot) is 0.9 m/s. Figure 19. (c) shows that in front of the conveyor at an amplitude of 0.1 T and 0.1 L with a speed of 1.028 m/s (2 knots) is 0.9 m/s (2 knots) is 1.108 m/s. Figure 19. (d) shows that in front of the conveyor at an amplitude of 0.5 T and a wavelength of 0.5L with a speed of 1.028 m/s (2 knots) is 1.551 m/s (2 knots). So that under the condition of amplitude 0.5 T and a wavelength of 0.5 L at a speed of 1.028 m/s (2 knots) is 1.551 m/s the fastest condition in collecting waste.

3.4 Effect of Wave Length and Height on Flow Patterns on Garbage Collection Vessels

In Figure 20. is the fluid flow pattern around the ship with two wave variations of 0.1 T and 0.1 L, 0.5 T and 0.5 L with two speeds of 0.514 m/s (1knot). and 1.028 m/s (2 knots). Figure 20. (a). speed 0.514 m/s (1 knot) with variations of 0.1 T and 0.1 L. Figure 20. (b). speed of 0.514 m/s (1 knot) with variations of 0.5T and 0.5L. Figure 20. (c). velocity of 1.028 m/s (2 knots) with variations of 0.1 T and 0.1 L.

Figure 20. (d). speed of 1.028 m/s (2knots) with variations of 0.5 T and 0.5 L. From Figure 20. (a) it can be seen that the direction of the fluid flow pattern in the direction of the direction is laminar and in the direction is turbulent. In the flow pattern there is a vector and *streamline*, the straight line indicates the direction of flow or *streamline* and the arrow indicates the vector. So that under the condition of amplitude 0.1 T and wavelength 0.1 L at a speed of 0.514 m/s (1 knot) is 0.7 m/s is easy to collect rubbish.

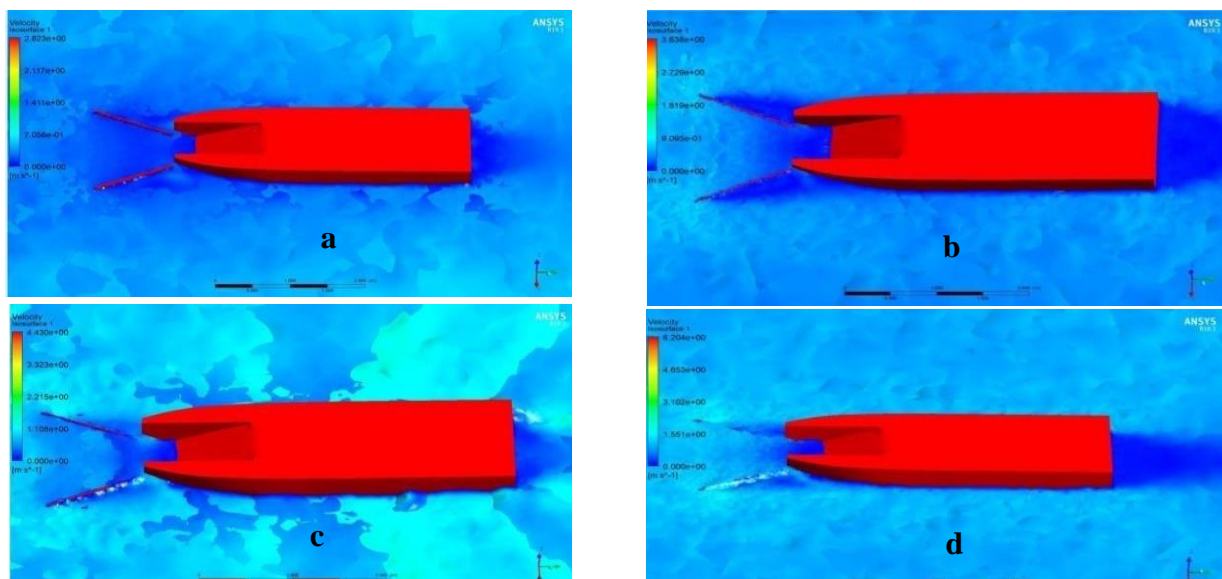


Figure 19. Comparison of speed contours of Top view (a) 0.1 T, 0.1 L at 1 knot (b) 0.5 T, 0.5 L at 1 knot (c) 0.1 T, 0.1 L at 2 knots. (d) 0.5 T and 0.5 L speed of 2 knots.

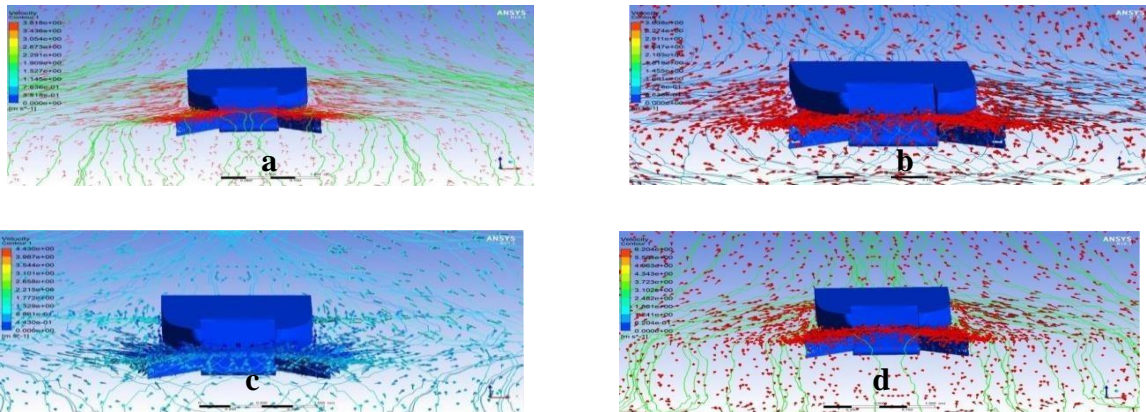


Figure 20. Flow pattern of front view (a) 0.1 T, 0.1 L at 1 knot (b) 0.5 T, 0.5 L at 1 knot (c) 0.1 T, 0.1 L at 2 knots (d) 0.5 T and 0.5 L at 2 knots.

In Figure 21. is the fluid flow pattern around the ship with two wave variations of 0.1 T and 0.1 L, 0.5 T and 0.5 L with two speeds of 0.514 m/s (1 knot). and 1.028 m/s (2 knots). Figure 21. (a). speed 0.514 m/s (1 knot) with variations of 0.1 T and 0.1 L. Figure 21. (b). speed of 0.514 m/s (1 knot) with variations of 0.5T and 0.5L. Figure 21. (c). speed of 1.028 m/s (2 knots) with variations of 0.1 T and 0.1 L. Figure 21. (d). speed 1.028 m/s (2 knots) with

variations of 0.5 T and 0.5 L. From Figure 21, it can be seen that the direction of the fluid flow pattern in the direction is laminar and in the direction is turbulent. In the flow pattern there is a vector and *streamline*, the straight line indicates the direction of flow or *streamline* and the arrow indicates the vector. So that under the condition of amplitude 0.5 T and wavelength 0.5 L at a speed of 0.514 m/s (1 knot) is 0.9 m/s is easy to collect rubbish.

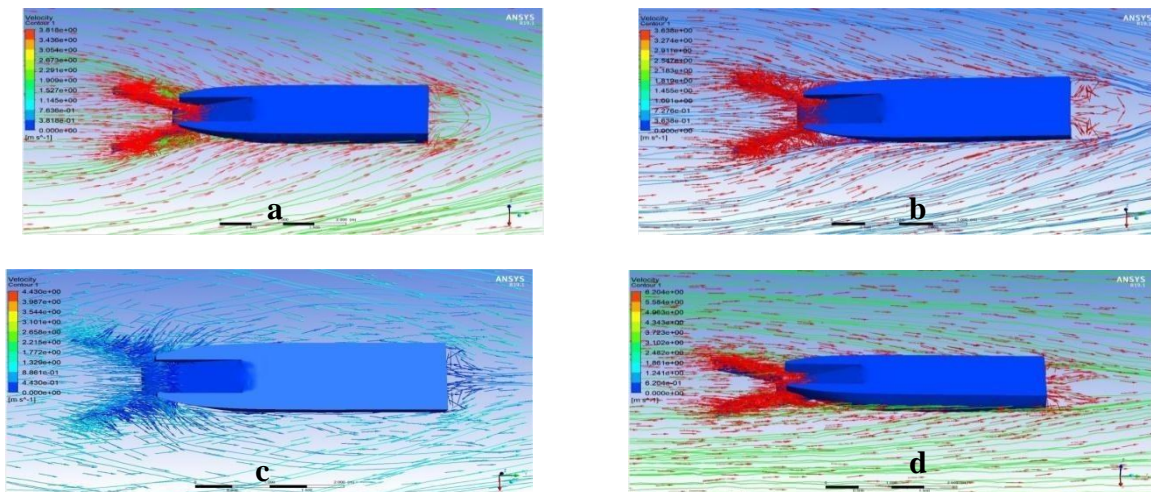


Figure 21. Flow pattern of top view (a) 0.1 T, 0.1 L at 1 knot (b) 0.5 T, 0.5 L at 1 knot (c) 0.1 T, 0.1 L at 2 knots (d) 0.5 T and 0.5 L at 2 knots.

In Figure 21. is the fluid flow pattern around the ship with two wave variations of 0.1 T and 0.1 L, 0.5 T and 0.5 L with two speeds of 0.514 m/s (1 knot). and 1.028 m/s (2 knots). Figure 21. (a). speed 0.514 m/s (1 knot) with variations of 0.1 T and 0.1 L. Figure 21. (b). speed of 0.514 m/s (1 knot) with variations of 0.5T and 0.5L. Figure 21. (c). speed of 1.028 m/s (2 knots) with variations of 0.1 T and 0.1 L. Figure 21. (d). speed 1.028 m/s (2 knots) with

variations of 0.5 T and 0.5 L. From Figure 21. (a) it can be seen that the direction of the fluid flow pattern in the direction is laminar and in the direction is turbulent. In the flow pattern there is a vector and *streamline*, the straight line indicates the direction of flow or *streamline* and the arrow indicates the vector. So that under the condition of amplitude 0.1 T and wavelength 0.1 L at a speed of 1.028 m/s (2 knots) are 1.108 m/s is easy to collect rubbish.

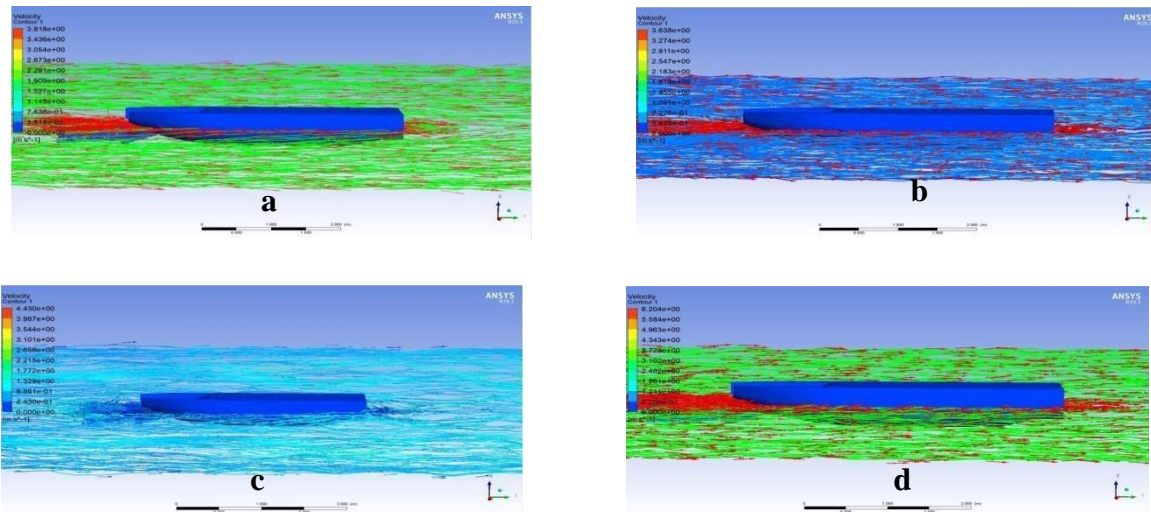
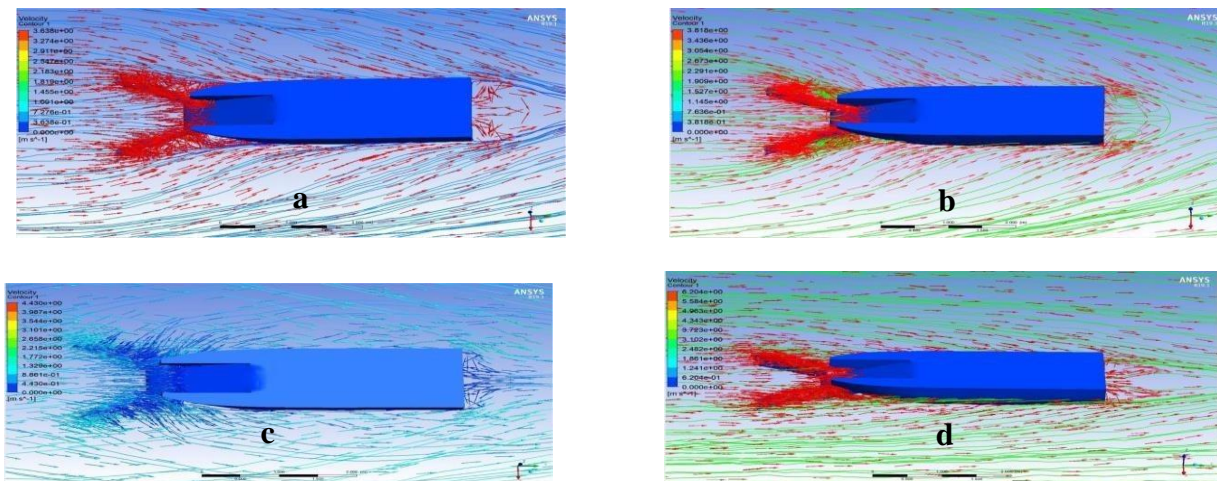


Figure 22. Flow pattern (a) 0.1 T, 0.1 L at 1 knot (b) 0.5 T, 0.5 L at 1 knot (c) 0.1 T, 0.1 L at 2 knots (d) 0.5 T and 0.5 L at 2 knots. Side view

3.5. Comparison of flow patterns with velocities of 0.514 m/s (1 knot) and 1.028 m/s (2 knots) with two wave variations of 0.1 T, 0.1 L and 0.5 T, 0.5 L

Figure 22 shows a comparison of flow patterns with two wave variations. In Figure (a), the speed of 0.514 m/s (1 knot) with wave variations of 0.1 T and 0.1 L is 0.7 m/s. Figure (b), the speed of 0.514 m/s (1 knot) with wave variations of 0.5 T and 0.5 L is 0.7 m/s.

0.9 m/s. Figure (c), the speed of 1.028 m/s (2 knots) with wave variations of 0.1 T and 0.1 L is 1.108 m/s. Figure (d), speed of 1.028 m/s (2 knots) with wave variations 0.5 T and 0.5 L is 1.551 m/s. So the model that has a laminar flow pattern at the bow and at the stern is Figure 22. (a) with a speed of 0.514 m/s (1 knot) at an amplitude variation of 0.1 T and a wavelength of 0.1 L is the best because it is easy to collect garbage.



Comparison of flow patterns with two wave variations of 0.1 T, 0.1 L and 0.5 T, 0.5 L and two velocities of 0.514 m/s (1 knot) and 1.028 m/s (2 knots) top view

In Figure 22, comparison of flow patterns with two wave variations in figures (a), (b), (c) and (d). It can be analysed that the model that has laminar flow patterns at the bow and at the stern is Figure 22. (a) with the speed of 0.514 m/s (1 knot) at the amplitude variation of 0.1 T and wavelength of 0.1 L is the best because it is easy to collect waste.

3.6. Ship resistance and effect on fuel emission in waste collection vessels

The following are the results of resistance from Ansys fluidflow (fluent) software simulations on the hollow wing conveyor ship model circle with 2 variations of wave length and amplitude and 2 variations of speed in Table 4.

TABLE 4.
 TOTAL RESISTANCE RESULTS

| Velocity (m/s) | Velocity variation (m/s) | Body sizing (mm) | Face sizing | Inflation mesh (layer) | Total element | Resistance (N) |
|----------------|--------------------------|------------------|-------------|------------------------|---------------|----------------|
| 0.514 | 0.1 L and 0.5 T | 350 | 250 | 15 | 1633329 | 3.0659 |
| 0.514 | 0.5 T and 0.5 L | 350 | 250 | 15 | 1633329 | 3.5268 |
| 1.028 | 0.1 T and 0.1 L | 350 | 250 | 15 | 1633329 | 18.9184 |
| 1.028 | 0.5 T and 0.5 L | 350 | 250 | 15 | 1633329 | 84.2143 |

In Figure 23. Shows the total resistance graph with two variations at an amplitude of 0.5 T and a wavelength of 0.5 L higher than at an amplitude of 0.1 T and

wavelength of 0.1 L. Then the higher the ship speed results in lower total resistance.

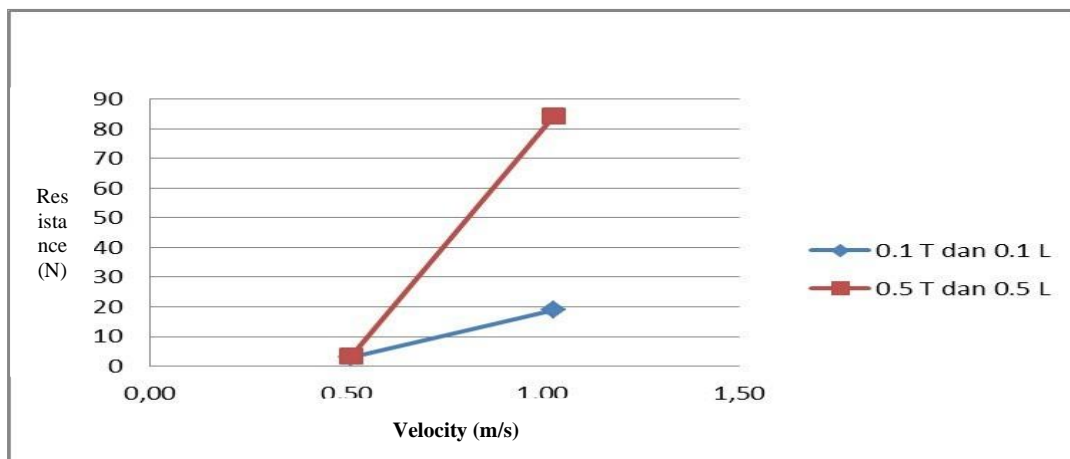


Figure 23. T total resistance

3.7. Validation of Simulation of Circular Hollow Wing Conveyance Ship Model with Experimental Trial

At the maximum speed of 0.514 m/s (1 knot). Waves generated due to interaction between the wings,

The water flow pattern before the bow has turbulence because the water is trapped between the wing and the conveyor so that it is pushed forward and the turbulence continues around the hull, especially at the stern.

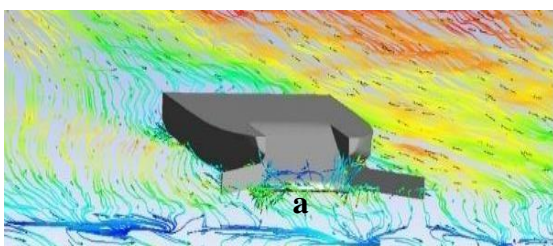


Figure 24: Water flow at 0.514 m/s (1 knot) (a) Ansys fluid fluent (b) experiment [14].

At the maximum speed of 1.028 m/s (2 knots). The waves generated due to the interaction between the conveyor wing, hull and water as shown in Figure 25. the water flow pattern before entering the bow hull has occurred.

Turbulence due to water trapped between the wing and conveyor is pushed forward and turbulence continues around the hull, especially at the stern.



Figure 25: Water flow at 1.028 m/s (2 knots) (a) Ansys fluid fluent (b) experiment [14].

3.8. Discussion

From the above research, it can be analysed that the effect of amplitude height on speed contours is that the higher the amplitude, the smaller the speed. This is evidenced from Figure 16. (a) which shows the effect of the length of the wave amplitude on the speed contour on the garbage collection ship at a speed of 0.514 m/s (1 knot) with a variation of wave height $0.1 T$ and wavelength $0.1 L$. Furthermore, the effect of length on speed is the longer the wave length, the greater the speed. This is evidenced from Figure 19. (d). which shows the analysis of the effect of the length of the wave amplitude on the speed contour on the garbage collection ship at a speed of 1.028 m/s (2 knots) with a wave height variation of $0.5 T$ and a wavelength of $0.5 L$.

The results of the velocity contours show that the higher the wave amplitude, the slower the garbage collection and the smaller the speed around the bow. Furthermore, the longer the wave length, the faster the garbage collection because the fluid velocity around the bow is greater.

The effect of amplitude height on the flow pattern is that the higher the amplitude, the more difficult it is for the ship to collect garbage. This is evidenced in Figure 22. which shows the analysis of the flow pattern on the garbage collection ship at a speed of 1.028 m/s with a wave amplitude variation of $0.5 T$ and a wavelength of $0.5 L$. Furthermore, the effect of wavelength on the flow pattern is the longer the wave, the easier it is to collect garbage. This is evidenced in Figure 20. about the flow pattern analysis of the flow pattern on the garbage collection ship with a speed of 0.514 m/s with a variation of $0.1 T$ wave amplitude and $0.1 L$ wavelength.

The results of the flow pattern show that the higher the wave amplitude, the more difficult the garbage collection is because the flow is shapeless and tends to be turbulent. Furthermore, the longer the wave length, the easier the garbage collection because the flow is laminar and this facilitates the collection of marine debris. The effect of wave length and amplitude on ship resistance is that the higher the wave amplitude, the greater the resistance. Likewise, the

Conversely, the lower the resistance, the lower the fuel longer the wave, the greater the ship's resistance.

This will affect fuel consumption. Because the higher the resistance, the greater the ship's power requirements. So the fuel consumption is also high. This affects operational costs which are increasingly expensive, consumption and the cheaper the operating costs.

IV. CONCLUSION

Based on the results of the study, the effect of length and amplitude of waves on waste collection vessels using *Computational Fluid Dynamic*, the best speed contour is at a speed of 2 knots. From the analysis of the circular hollow wing at a variation of $0.5 T$ amplitude and $0.5 L$ wavelength has the highest velocity contour with a value of 1.551 m/s at the bow and at the stern. Then, the model that has a laminar flow pattern at the bow and at the stern is a speed of 0.514 m/s (1 knot) at an amplitude variation of $0.1 T$ and a wavelength of $0.1 L$. This is the best because it is easy to collect garbage.

The smallest drag was at a speed of 0.514 m/s (1 knot) at an amplitude variation of $0.1 T$ and wavelength of 0.514 m/s (1 knot). $0.1 L$. So that at the speed of $0.1 T$ amplitude variation and $0.1 L$ wavelength, the fuel speed is less. Furthermore, the greater the wavelength and the higher the wave amplitude, the greater the ship's resistance and the smaller the speed. The minimum assumption at $0.1 T$ amplitude variation, $0.1 L$ wavelength is easier to collect garbage and the maximum at $0.5 T$ amplitude variation, $0.5 L$ wavelength is faster to collect garbage.

Future research can be carried out simulating perfect *meshing*, so that the results can be perfect according to the standard. Furthermore, for the speed and variation of waves can be added with a speed of $1, 2, 3, 4 \text{ m/s}$ and the variation can use $1 L, 1 T, 2 L, 2 T, 3 L, 3 T, 4 L, 4 T$. Then, further research needs to be done experimentally in towing tanks. And prototyping also needs to be done to conduct stability tests, and ship motion.

ACKNOWLEDGEMENT

The author would like to thank the Ministry of Research and Technology of the Republic of Indonesia for providing basic research funding through the Penelitian Dosen Pemula (PDP) scheme program based on Contract Agreement Number 183/E5/PG.02.00.PL/2023, 032/SP2H/PT/LL7/2023, and B/09/HIB-EX.PB/UHT.C7/VI/2023.

REFERENCES

- [1] Chiba, S., Saito, H., Fletcher, R., Yogi, T., Kayo, M., Miyagi, S., ... & Fujikura, K. (2018). Human footprint in the abyss: 30-year records of deep-sea plastic debris. *Marine Policy*, 96, 204-212. <https://doi.org/10.1016/j.marpol.2018.03.022>
- [2] Pradit, S., Noppradit, P., Loh, P. S., Nitiratsuwan, T., Le, T. P. Q., Oeurng, C., ... & Wang, J. (2022). The Occurrence of microplastics in sediment cores from two mangrove areas in southern Thailand. *Journal of Marine Science and Engineering*, 10(3), 418. <https://doi.org/10.3390/jmse10030418>
- [3] World Bank Group. (2018). *Indonesia's Marine Debris Hotspot*; World Bank Group: Jakarta, Indonesia.
- [4] Leal Filho, W., Hunt, J., & Kovaleva, M. (2021). Garbage patches and their environmental implications in a plastic sphere. *Journal of Marine Science and Engineering*, 9(11), 1289. <https://doi.org/10.3390/jmse9111289>
- [5] Sugianto, E., & Jeng-Horng, C. (2021). 'Buy Marine Debris': A Digital Platform for Sustainable Marine Debris Management Involving Fishermen. *Nusantara: An International Journal of Humanities and Social Sciences*, 3(1), 36-48. [https://www.airitilibrary.com/Common/Click_DOI?DOI=10.6936/NIJHSS.202106_3\(1\).0003](https://www.airitilibrary.com/Common/Click_DOI?DOI=10.6936/NIJHSS.202106_3(1).0003)
- [6] Sugianto, E., Zamzami, R. A., Winarno, A., & Prasutiyon, H. (2022). Effect of Catamaran Hull Type on Ocean Waste Collection Behavior. *Journal of Marine-Earth Science and Technology*, 3(3), 79-85. <https://doi.org/10.12962/j27745449.v3i3.590>
- [7] Sugianto, E.; Chen, J.H. (2019). Preliminary concept of ship use to waste management in shallow sea water. In *Proceedings of the 33th Asian-Pacific Technical Exchange and Advisory Meetings on Marine Structures (TEAM 2019)*, Tainan, Taiwan, 14-17 October 2019.
- [8] Sugianto, E., Chen, J. H., & Purba, N. P. (2023). Cleaning technology for marine debris: A review of current status and evaluation. *International Journal of Environmental Science and Technology*, 20(4), 4549-4568. <https://doi.org/10.1007/s13762-022-04373-8>
- [9] Sugianto, E.; Chen, J.H.; Purba, N.P. (2021). Numerical investigation of conveyor wing shape type effect on ocean waste collection behaviour. *E3S Web Conf.*, 01005. <https://doi.org/10.1051/e3sconf/202132401005>
- [10] Sugianto, E., Chen, J.-H., Sugiono, R., & Prasutiyon, H. (2022). Effect of portable conveyor placement in ship on ocean waste collection behaviour. *IOP Conference Series: Earth and Environmental Science*, 1095(1), 012015. <https://doi.org/10.1088/1755-1315/1095/1/012015>
- [11] Sugianto, E., Chen, J. H., & Permadi, N. V. A. (2022). Effect of Monohull Type and Catamaran Hull Type on Ocean Waste Collection Behaviour Using OpenFOAM. *Water*, 14(17), 2623. <https://doi.org/10.3390/w14172623>
- [12] Ihsani, N., and Sugianto, E. (2022). Effect of hole shape on the conveyor wing of the waste collection ship on the effectiveness of waste collection using Computational Fluid Dynamic (CFD). *Hang Tuah University*.
- [13] BMKG, (2023). *BMKG Weather Forecast. Surabaya Region*.
- [14] Sugianto, E., & Chen, J. H. (2022). Experimental Study of the Effect of a Solid Wing Conveyor on Marine Debris Collection. *Journal of Marine Science and Technology*, 30(6). <https://doi.org/10.51400/2709-6998>